Article

The Kinetics of Helix Unfolding of an Azobenzene Cross-Linked Peptide Probed by Nanosecond Time-Resolved Optical Rotatory Dispersion

Eefei Chen, Janet R. Kumita, G. Andrew Woolley, and David S. Kliger

J. Am. Chem. Soc., **2003**, 125 (41), 12443-12449• DOI: 10.1021/ja030277+ • Publication Date (Web): 19 September 2003

J|A|C|S
ARTICLES
Published on Web 09/19/2003

The Kinetics of Helix Unfolding of an Azobenzene Cross-Linked Peptide Probed by Nanosecond Time-Resolved Optical Rotatory Dispersion

Eefei Chen,[†] Janet R. Kumita,[‡] G. Andrew Woolley,[‡] and David S. Kliger*,[†]

Contribution from the University of California, Department of Chemistry and Biochemistry, Santa Cruz, California 95064, and University of Toronto, Department of Chemistry, 80 Saint George Street, Toronto M5S 3H6, Canada

Received May 6, 2003; E-mail: kliger@chemistry.ucsc.edu

Abstract: The unfolding dynamics of a 16 amino acid peptide (Ac-EACAREAAAREAACRQ-NH_2, FK-11-X) was followed using nanosecond time-resolved optical rotatory dispersion (ORD). The peptide was coupled to an azobenzene linker that undergoes subnanosecond photoisomerization and reisomerizes on a time scale of minutes. When the linker is in the *trans* form, the peptide favors a more helical structure (66% helix/34% disordered) and when in the *cis* configuration the helical content is reduced. Unfolding of FK-11-X was rapidly triggered by a 7-ns laser pulse at 355 nm, forming *cis* azobenzene-linked peptides that maintained the secondary structure (helical or disordered) of their *trans* azobenzene counterparts. The incompatibility of the instantaneous *cis* photoproduct with helical secondary structure drives the subsequent peptide unfolding to a new conformational equilibrium between *cis* helix and *cis* disordered structures. The kinetic results show a ~40% decrease in the time-dependent ORD signal at 230 nm that is best fit to a single-exponential decay with a time constant of 55 ± 6 ns. Folding and unfolding rates for *cis* FK-11-X are estimated to be ~3.0×10^6 s^{-1} (1/330 ns) and ~1.5×10^7 s^{-1} (1/66 ns), respectively.

Introduction

One of the fundamental issues for biophysics is to develop an understanding of how proteins fold to their native structures. To fully address this issue it is necessary to explore not only the energetics of folding but also the dynamics of folding. In exploring folding dynamics it is useful to study the folding of naturally occurring proteins, as well as the folding in model polypeptide systems, to understand the factors that control the dynamics of secondary structure formation. For relatively short helical polypeptides secondary structure formation is expected to occur in the submicrosecond time regime. Thus, to study the kinetics of these processes one must not only have fast spectroscopic probes capable of distinguishing helical structure from random coil structures, but one must also be able to trigger the folding process on a nanosecond time scale. Some of the more common protein folding triggers include fast temperature (T-jump),[1] pH,[2] and pressure jumps,[3] ligand photodissociation,[4] electron transfer,[5] and rapid mixing.[6] Fast peptide dynamics have typically been initiated with a T-jump trigger.

A different approach to initiate peptide folding involves synthesis of peptides incorporating photoactive molecules.[7−17] This approach offers the ability to reversibly and more finely control secondary structure content. For example, when a photocleavable aryl disulfide cross-linker was incorporated into a helical, polyalanine peptide a 2-fold decrease in helicity was observed.[11] Similarly, in the presence of a 3′-(carboxymethoxy)-benzoin (CMB) group an initially randomly structured, cyclic peptide formed helix structure upon irradiation.[13] The use of an aromatic amide derivative of a tris-bipyridyl complex

[†] University of California.
[‡] University of Toronto.

(1) Callender, R.; Dyer, R. B. *Curr. Opin. Struct. Biol.* **2002**, *12*, 628.
(2) Abbruzzetti, S.; Viappiani, C.; Small, J. R.; Libertini, L. J.; Small, E. W. *J. Am. Chem. Soc.* **2001**, *123*, 6649.
(3) Jacob, M.; Holtermann, G.; Perl, D.; Reinstein, J.; Schindler, T.; Geeves, M. A.; Schmid, F. X. *Biochemistry* **1999**, *38*, 2882.
(4) Jones, C. M.; Henry, E. R.; Hu, Y.; Chan, C.-K.; Luck, S. D.; Bhuyan, A.; Roder, H.; Hofrichter, J.; Eaton, W. A. *Proc. Natl. Acad. Sci. U.S.A.* **1993**, *90*, 11860.
(5) (a) Pascher, T.; Chesick, J. P.; Winkler, J. R.; Gray, H. B. *Science* **1996**, *271*, 1558. (b) Mines, G. A.; Pascher, T.; Lee, S. C.; Winkler, J. R.; Gray, H. B. *Chem. Biol.* **1996**, *3*, 491.
(6) Shastry, M. C. R.; Luck, S. D.; Roder, H. *Biophys. J.* **1998**, *74*, 2714.
(7) (a) Pieroni, O.; Houben, J. L.; Fissi, A.; Costantino, P.; Ciardelli, F. *J. Am. Chem. Soc.* **1980**, *102*, 5913. (b) Pieroni, O.; Fissi, A.; Houben, J. L.; Ciardelli, F. *J. Am. Chem. Soc.* **1985**, *107*, 2990. (c) Pieroni, O.; Fissi, A.; Angelini, N.; Lenci, F. *Acc. Chem. Res.* **2001**, *34*, 9.
(8) Ciardelli, F.; Fabbri, D.; Pieroni, O.; Fissi, A. *J. Am. Chem. Soc.* **1989**, *111*, 3470.
(9) Ulysse, L.; Cubillos, J.; Chmielewski, J. *J. Am. Chem. Soc.* **1995**, *117*, 8466.
(10) Cerpa, R.; Cohen, F. E.; Kuntz, I. D. *Folding Des.* **1996**, *1*, 91.
(11) (a) Lu, H. S. M.; Volk, M.; Kholodenko, Y.; Gooding, E.; Hochstrasser, R. M.; DeGrado, W. F. *J. Am. Chem. Soc.* **1997**, *119*, 7173. (b) Volk, M.; Kholodenko, Y.; Lu, H. S. M.; Gooding, E. A.; DeGrado, W. F.; Hochstrasser, R. M. *J. Phys. Chem. B* **1997**, *101*, 8607.
(12) (a) Behrendt, R.; Renner, C.; Schenk, M.; Wang, F.; Wachtveitl, J.; Oesterhelt, D.; Moroder, L. *Angew. Chem., Int. Ed.* **1999**, *38*, 2771. (b) Renner, C.; Behrendt, R.; Spörlein, S.; Wachtveitl, J.; Moroder, L. *Biopolymers* **2000**, *54*, 489. (c). Renner, C.; Cramer, J.; Behrendt, R.; Moroder, L. *Biopolymers* **2000**, *54*, 501.
(13) Hansen, K. C.; Rock, R. S.; Larsen, R. W.; Chan, S. I. *J. Am. Chem. Soc.* **2000**, *122*, 11567.
(14) Huang, C.-Y.; He, S.; DeGrado, W. F.; McCafferty, D. G.; Gai, F. *J. Am. Chem. Soc.* **2002**, 124, 12674−12675.
(15) Ueno, A.; Takahashi, K.; Anzai, J.-I.; Osa, T. *J. Am. Chem. Soc.* **1981**, *103*, 6410.
(16) Kumita, J. R.; Smart, O. S.; Woolley, G. A. *Proc. Natl. Acad. Sci. U.S.A.* **2000**, *97*, 3803.
(17) Flint, D. G.; Kumita, J. R.; Smart, O. S.; Woolley, G. A. *Chem. Biol.* **2002**, *9*, 391.

([Rub_2m-OH]$^{2+}$) as a peptide capping group led to stabilization of helical conformation after a photoinduced charge generation event.[14] The CD spectra for poly(L-glutamic acid) show the formation of α-helix from random coil structure upon closed-to-open ring interconversion of appended spiropyran units induced by visible light.[8] Azobenzene groups have been successfully used to modulate the conformation of cyclic peptides,[9,12] the sense of a peptide helix,[15] the changes in peptide aggregation,[7b] and the content of peptide helix, β-sheet, and coil structures.[7a,10,16,17]

In designing a photoisomerizable cross-linking strategy for folding/unfolding studies there are several desirable properties to consider. The sensor molecule should undergo its light-induced response on a time scale faster than, and distinguishable from, the folding or unfolding reaction. A high photoproduct yield for both the isomerization of the sensor and the peptide structural change, as well as a slow reversibility of the reaction, enhances the signal-to-noise of the experiment. Finally, the use of water as the solvent is desirable for understanding protein/peptide folding under physiological conditions. The success of a cross-linked peptide for kinetic studies requires that many of these conditions work together optimally. Low photoproduct yield of the photoactive group, rapid reversibility of the photoinitiation event, and irreversibility of the reaction are some of the experimental challenges that have been observed during kinetic measurements of these peptide systems. Recently, however, Kumita et al.[16] and Flint et al.[17] introduced an azobenzene-based cross-linker that could be linked to two cysteine residues in a peptide. When the cysteines occupy an *i*, $i + 4$ spacing, a *trans*-to-*cis* photoisomerization of the cross-linker leads to an increase in helix content by 38%. With an *i*, $i + 11$ spacing of the cysteines, a 40% decrease in helical structure is observed upon continuous wave (CW) illumination of the *trans* cross-linked peptide with 370 nm light.

In this study we use nanosecond time-resolved optical rotatory dispersion (TRORD) measurements to follow the unfolding of the peptide with *i*, $i + 11$ cysteine spacing described by Flint et al. (FK-11-X)[17] after photoisomerization of the azobenzene cross-linker. The kinetic results show a ~40% decrease in the ORD signal at 230 nm that is best fit to a single-exponential decay with a time constant of 55 ± 6 ns.

Materials and Methods

Sample Preparation. The FK-11-X peptide was designed and prepared according to the methods described by Flint et al.[17] The azobenzene moiety was cross-linked to the peptide between two cysteines at positions 3 and 14 in the sequence (Ac-EACAREAAAR-EAACRQ-NH_2).

Tris(2,2′-bipyridyl)ruthenium(II) chloride hexahydrate ($Ru(bpy)_3Cl_2$) was purchased from Aldrich Chemical Co., and monobasic and dibasic sodium phosphates were purchased from Fisher Scientific. All were used without further purification.

For the time-resolved experiments lyophilized peptide was dissolved in 5 mM sodium phosphate buffer (pH 7) to obtain samples with an OD_{230} of ~0.6 (157 μM) for TRORD experiments and an OD_{362} of ~0.7 (125 μM) for TROD experiments. TROD studies of $Ru(bpy)_3Cl_2$ were performed on samples prepared in water with an OD_{285} of ~0.8. The final volume of peptide sample used for all TROD and TRORD experiments was ~3 mL.

Time-Resolved Experiments. The TRORD apparatus for far-UV spectral detection was modified from the TRCD configuration described in 1993 by Zhang et al.[18] to allow for experiments on small sample volumes. Photoisomerization of the azobenzene group was initiated by a 2-mJ pulse of 355 nm light (7 ns, fwhm) that was generated by a Q-switched Quanta Ray DCR-1 Nd:YAG laser (Spectra-Physics, Mountain View, CA). The laser beam passed through the sample at approximately 20° relative to the probe beam, which was oriented at 90° to the face of the sample cell. The probe beam was initially unpolarized light from a xenon flashlamp, but was converted to linearly polarized light upon passing through a MgF_2 polarizer. The sample cell was placed after the first polarizer and before a second polarizer that was positioned with its polarization axis oriented at $90° + \beta$, where $\beta = \pm 1.88°$ for ORD measurements. Changes in the polarization properties of the probe light which passed through the sample were observed by a spectrograph that was equipped with a 2-mm slit and a 600 g/mm grating blazed at 200 nm and an optical multichannel analyzer (OMA) detector. The TRORD system was designed to allow data collection on small sample volumes. By placing two mirrors between the two polarizers that were oriented at nearly 90°, the probe light was focused down from the initial 6-mm to a 300-μm beam diameter. The probe beam was overlapped at the sample with the laser beam, which was focused down to a ~1-mm diameter.

For TRORD experiments signals were measured at 50, 60, 80, 90, 130, 160, 640, and 990 ns and 10, 100 and 500 μs and 1 ms after photoinitiation of peptide unfolding. An initial state spectrum of the FK-11-X peptide was measured before each time-resolved point. Approximately 246 averages were collected for each time point, with the exception of 50 ns for which 120 averages were accumulated.

The TROD measurements were obtained on the TRORD apparatus, but with the first polarizer turned ~6° off the crossed position (90°) relative to the second polarizer. To establish the time resolution of the OD experiments, measurements were made on the triplet formation and decay of $Ru(bpy)_3Cl_2$. TROD data for FK-11-X were measured in both the mid-UV (260−300 nm) and the near UV to visible (320−420 nm) regions, whereas TROD data for $Ru(bpy)_3Cl_2$ were measured only from 210 to 300 nm. Forty-eight averages were collected at each time delay (10, 20, 30, 40, 50, 100, 130, 610, and 960 ns and 10 and 100 μs) for FK-11-X TROD experiments. $Ru(bpy)_3Cl_2$ measurements were made at 10 delay times per decade from 10 ns to 1 μs and then at 2, 5, 10, 50, 100, and 500 μs and 1 ms.

TROD measurements on the 267- and 360-nm bands were important because they represent the $\pi-\pi^*$ transitions for the *cis* and *trans* forms, respectively, of the azobenzene group alone.[19] Data in these regions were necessary to distinguish between the kinetics of photoisomerization and those of peptide unfolding. Unfortunately, 355-nm laser scatter interferes with the data at the earliest times for the 360-nm band. By using a 3-75 filter (410 nm, Corning, NY) to cut out the 355-nm light it was possible to collect TROD data at the red tail (380 to 460 nm) of the 360-nm band.

All experiments were performed in the dark at ~25 °C. Because the half-life of thermal relaxation for FK-11-X is ~12 min at 25 °C,[17] it was not possible to continually recycle the sample. Thus, a peristaltic pump was used to cycle the peptide sample to a 2-mm path length flow cell and then to a collection vial that was maintained at 37 °C. At this temperature the thermal relaxation half-time is ~3 min. Before the sample was reused a UV−vis absorption spectrum (Shimadzu UV-2101PC, Columbia, MD) of the peptide was measured and compared to the spectrum of the peptide measured prior to the experiments. The laser repetition rate was 0.5 Hz so that sample could be flowed (4.6 μL/s) between laser shots to avoid photoproduct build-up.

Data Analysis. TROD and TRORD data were analyzed in the form of difference spectra, calculated by subtracting the initial state spectrum from each time-delayed photoproduct spectrum. Singular-value decomposition (SVD) and global exponential fitting were used to

(18) Zhang, C. F.; Lewis, J. W.; Cerpa, R.; Kuntz, I. D.; Kliger, D. S. *J. Phys. Chem.* **1993**, *97*, 5499.
(19) Hamm, P.; Ohline, S. M.; Zinth, W. *J. Chem. Phys.* **1997**, *106*, 519.

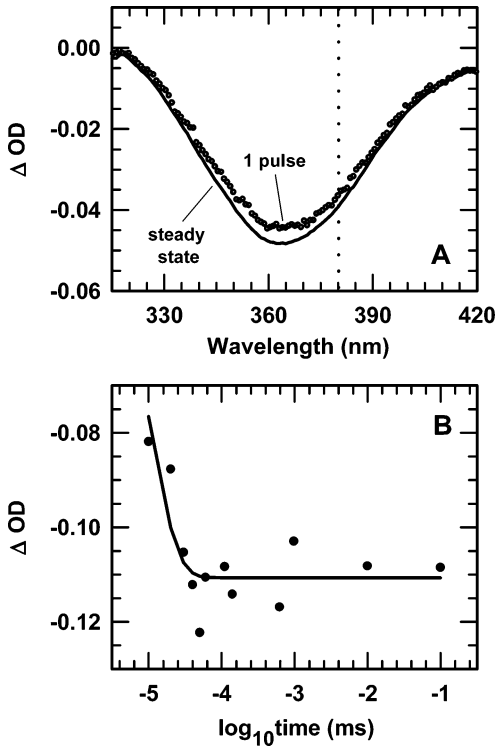

Figure 1. Repetitively pulsed steady-state absorption and TROD data for FK-11-X in the visible region (360 nm). (A) The difference (*cis* photoproduct − initial *trans*) absorption spectrum of the *cis* FK-11-X photoproduct formed after 1 pulse of 355 nm (dotted) is ~90% of the steady-state difference spectrum (solid) formed by repetitively pulsed irradiation. (B) The difference TROD data for the 360-nm band is measured from 380 (indicated by the dotted line in (A)) to 460 nm because of 355-nm laser scatter. The kinetic data at 390 nm can be fit well to a single exponential with a time constant of 7 ± 2 ns.

determine the time-dependent behavior of the multiwavelength data. Exponential fitting analyses were also performed on "kinetic" traces, which were obtained from the multiwavelength data by averaging signals in a 4-nm window around the wavelength peak of interest. All algorithms for analyses were written with the mathematical software package Matlab (Pro-Matlab, The Mathworks Inc., South Natick, MA). Readers are directed to a previously published, detailed description of SVD and global analyses of kinetic spectral data.[20]

Results

Figure 1A shows that the difference absorption spectrum of the *cis*-FK-11-X generated by 1 pulse of 2 mJ, 355-nm light is ~90% of the steady-state spectrum formed by repetitively pulsed 355-nm irradiation of the *trans* peptide. Using the extinction coefficients at 362 nm for the *trans* (ϵ = 27 881 M^{-1} cm^{-1}) and *cis* (ϵ = 1382 M^{-1} cm^{-1}) peptides, the *cis*-FK-11-X yield in the single-pulse TROD experiments is calculated to be ~50%. The lower yield for 355 nm versus 370 nm (80%)[17] irradiation is attributed to the greater *cis*-to-*trans* back photoreaction arising from the larger extinction coefficient for the *cis* form at 355 nm (ϵ = 2456.7 M^{-1} cm^{-1}) than at 370 nm (ϵ = 870.5 M^{-1} cm^{-1}).

The TROD experiments in this region were localized to the red tail (380−460 nm, see Figure 1A) of the 360-nm band to avoid 355-nm laser scatter. These data were offset to zero at wavelengths longer than 460 nm where the UV−vis spectra show less than 6% change in absorption upon CW irradiation of *trans*-FK-11-X with 370-nm light.[17] This change will be even smaller, and within the noise level of our experiment, due to the smaller photoproduct yield from 355-nm (versus 370-nm) irradiation.

Figure 1B shows the kinetic trace obtained by averaging the multiwavelength TROD data (not shown) from 388 to 392 nm. These data are best fit to a single-exponential process with a time constant of 7 ± 2 ns. Previous time-resolved absorption studies of azobenzene photoisomerization have reported femtosecond formation of the excited state of *cis*-azobenzene and vibrational relaxation to the ground state in a few picoseconds in hexane, cyclohexane, and hexadecane.[21] In ethanol, formation of the excited state of *cis*-azobenzene was observed in 320 fs and vibrational cooling to the ground state in 2 ps.[22] Given the kinetic results of azobenzene photoisomerization in the various solvents, it seems unlikely that azobenzene photoisomerization in water would be 3 orders of magnitude slower. However, to test if a slower apparent isomerization is due to attachment of the azobenzene to the peptide or simply represents our instrument response time, TROD studies were performed on Ru(bpy)$_3$Cl$_2$. This molecule was chosen because the kinetics of the excited state are well characterized, with formation of the triplet state after 436 nm excitation in less than 100 ps[23] and decay of the long-lived triplet state in 580 ns (H_2O, 25 °C).[24]

The results of TROD studies on Ru(bpy)$_3$Cl$_2$ in the UV region (220−305 nm) are shown in Figure 2A. To assess the variability of the exponential fits to the data as a function of wavelength, kinetic traces were obtained at 232, 259, and 285 nm. The resulting exponential fits are shown with the corresponding data in Figure 2B. At each wavelength the kinetic traces can be fit to two exponential processes: 9 ± 2 and 350 ± 20 ns at 285 nm, 16 ± 2 and 400 ± 15 ns at 259 nm, and 16 ± 2 and 420 ± 20 ns at 232 nm. The long time component (~400 ns) is consistent with the reported lifetime of the triplet-state decay.[24] However, the 9 and 16 ns processes cannot be due to triplet-state formation, which occurs on the early picosecond time scale.[23] This fast component and the 7 ns time constant reported by the above TROD studies of FK-11-X near 360 nm are thus assigned to the rise time of the time-resolved apparatus.

Because the TROD data in the visible region were collected on only part of the 360 nm band, TROD data were also measured in the near-UV region. The 267 nm band reflects only the dynamics of the azobenzene moiety because the peptide does not contain aromatic amino acids. The data were offset to zero at 249 nm, an isosbestic point.[17] Figure 3 shows the kinetic trace obtained from the multiwavelength TROD data collected on the 267 nm band (inset). In the inset only the OMA data measured at 10 ns and 10 μs after the photoisomerization event are shown. The time-dependent behavior of the data is best fit with a single-exponential process having a lifetime of 16 ± 1 ns. This 16 ns process correlates with the rise time of the instrument, as suggested by the 16 ns component that was fit to the 259 nm kinetic trace for Ru(bpy)$_3$Cl$_2$ (Figure 2) and

(20) Goldbeck, R. A.; Kliger, D. S. *Methods Enzymol.* **1993**, *226*, 155.

(21) (a) Lednev, I. K.; Ye, T.-Q.; Hester, R. E.; Moore, J. N. *J. Phys. Chem.* **1996**, *100*, 13338. (b) Lednev, I. K.; Ye, T.-Q.; Matousek, P.; Towrie, M.; Foggi, P.; Neuwahl, F. V. R.; Umapathy, S.; Hester, R. E.; Moore, J. N. *Chem. Phys. Lett.* **1998**, *290*, 68.

(22) Nägele, T.; Hoche, R.; Zinth, W.; Wachtveitl, J. *Chem. Phys. Lett.* **1997**, *272*, 489.

(23) (a) Carroll, P. J.; Brus, L. E. *J. Am. Chem. Soc.* **1987**, *109*, 7613. (b) Chang, Y. J.; Orman, L. K.; Anderson, D. R.; Yabe, T.; Hopkins, J. B. *J. Chem. Phys.* **1987**, *87*, 3249.

(24) Van Houten, J.; Watts, R. J. *J. Am. Chem. Soc.* **1976**, *98*, 4853.

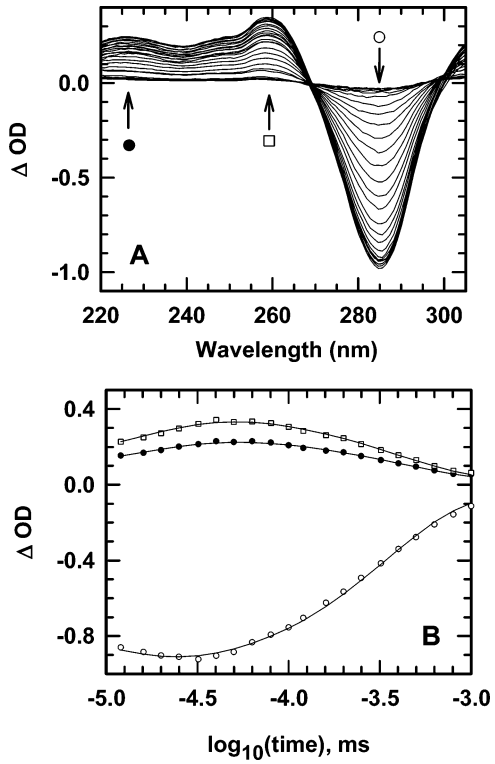

Figure 2. TROD data for $Ru(bpy)_3Cl_2$ in the 220−305-nm spectral region. The TROD data measured at 27 time delays after excitation with 2-mJ, 355-nm light are shown in (A). In (B) the kinetic traces for each of the wavelengths indicated in A are shown with two exponential fits to the data: 16 ± 2 and 420 ± 20 ns at 232 nm, 16 ± 2 and 400 ± 15 ns at 259 nm, and 9 ± 2 and 350 ± 20 ns at 285 nm.

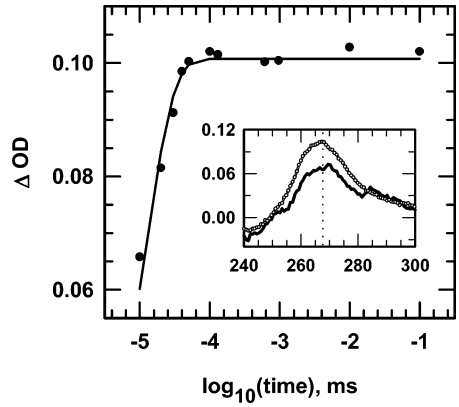

Figure 3. TROD data for FK-11-X in the near UV region (267 nm). The kinetic trace for the absorption band at 267 nm (inset) is best fit to a single-exponential process with a time constant of 16 ± 1 ns. The inset shows difference absorption spectra of the *cis* peptide 10 ns (black) and 10 μs (circles) after photoexcitation.

is consistent with the conclusions of TROD studies on the 360 nm band. These TROD studies on the 360 and 267 nm bands indicate that azobenzene photoisomerization is complete within 16 ns.

To probe the kinetics of peptide unfolding in FK-11-X far-UV TRORD data were measured. Figure 4A shows the multiwavelength data for the initial *trans*-FK-11-X peptide and the *cis* photoproducts measured at 60 ns and 10 μs. Only two time-delayed signals (out of 12) are shown to emphasize the major aspects of the ORD changes. A kinetic trace (232 nm) of all the difference ORD data from 50 ns to 10 μs is shown in Figure 4B. The time-dependent behavior of the TRORD data

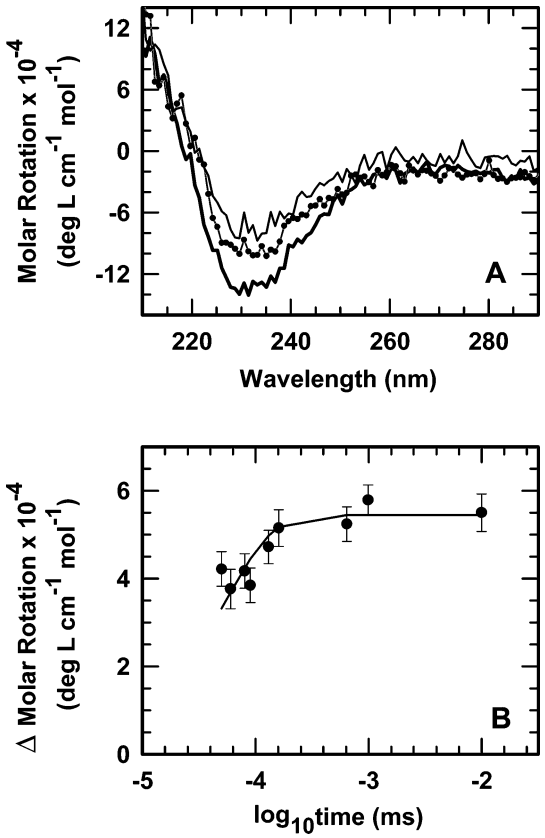

Figure 4. Far-UV TRORD data (232 nm band) for FK-11-X. In (A) the ORD signal for the initial *trans* peptide (heavy black) is compared to the signals measured at 60 ns (dotted) and 10 μs (thin black). Only two time-delayed signals are shown to emphasize the major changes. A kinetic trace (232 nm) of the difference TRORD data with time delays from 50 ns to 10 μs is shown in (B) along with a single-exponential fit (τ = 55 ± 6 ns) to the data. The data measured at 100 and 500 μs and 1 ms are not significantly different from the 10 μs point and are not shown.

is best fit to a single-exponential process with a time constant of 55 ± 6 ns. TRORD data at 100 and 500 μs and 1 ms do not show any further decrease in the magnitude of the ORD signal relative to 10 μs and are therefore not shown. Because the rise time of the instrument was shown to be 16 ± 2 ns in the 232-nm wavelength region, it is reasonable that the 55 ± 6 ns process can be assigned to the unfolding kinetics of the peptide.

Discussion

In this study we use a 16 amino acid peptide system that incorporates an azobenzene linker which undergoes subnanosecond photoisomerization and then thermally reisomerizes (*cis* → *trans*) on a time scale of minutes. The peptide adopts a helical structure when the linker is in the *trans* form and takes on a less helical conformation when the azobenzene is in the *cis* form. Illumination of the *trans* azobenzene in the highly helical FK-11-X leads to substantial formation of disordered structure, as characterized by their respective equilibrium CD spectra.[17] The sum of these design specifications allows us to rapidly trigger unfolding through the photoisomerization event without interference from refolding events on the time scale of the experiments and to minimize misinterpretation of the dynamics of the trigger event for peptide unfolding. In addition, because the initial *trans* peptide is regained after minutes,[17] it was possible to perform all the TROD and TRORD studies on only 3 mL of sample.

Scheme 1

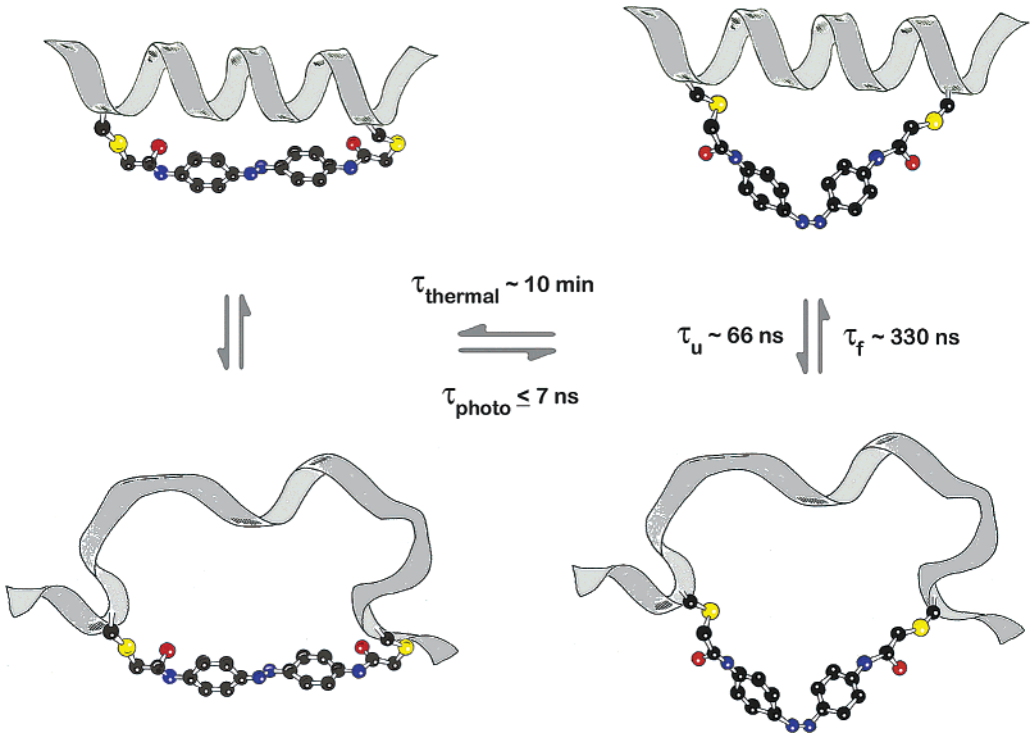

The TRORD changes following rapid photoisomerization of FK-11-X (Figure 4A) are associated with a decrease in helical conformation upon formation of the *cis* peptide. This assignment is made largely because the time-dependent spectral changes are similar to the equilibrium ORD signals obtained by a Kramers−Kronig transformation of the CD spectra shown in Flint et al. (Figure 6b)[17] of the peptide before and after illumination. The time-dependent behavior of the TRORD data is best fit to a single-exponential process with a time constant of 55 ± 6 ns, which is significantly greater than the 16 ± 2 ns process that has been identified as the rise time of the time-resolved apparatus. Because the TRORD experiments were performed at 25 °C where the half-life for thermal relaxation of the *cis* azobenzene chromophore is 12.3 ± 0.3 min,[17] the *cis* → *trans* reisomerization back reaction is considered negligible.

The 55 ns time constant is expected to reflect the unfolding dynamics for only the *cis*-FK-11-X peptide. Upon irradiation sequential photon events during the 7-ns width of the 2-mJ laser pulse result in multiple interconversions of the *trans* and *cis* forms. Within this time the peptide does not undergo major secondary structural changes so that immediately after the 7-ns photoevent the *cis* peptides that are formed will maintain the structure initially adopted by their *trans* counterparts—that is, either highly helical or disordered. The incompatibility of the instantaneous *cis* photoproduct with a helical secondary structure drives the subsequent peptide unfolding to a new conformational equilibrium between the *cis* helix and the *cis* disordered structures. The 55-ns relaxation kinetics must then reflect a sum of the rates of folding and unfolding within the *cis* peptide configuration if the system can be adequately described by two states. Scheme 1 provides an overview of the kinetic processes described above.

To determine the contributions of the folding and unfolding rates to the observed relaxation kinetics it is necessary to have an equilibrium constant for *cis* peptide unfolding. In the absence of temperature-dependent CD or ORD data an equilibrium constant is estimated from the percentages of helix and disordered structures in FK-11-X observed after 370-nm irradiation. According to measurements of equilibrium absorption and CD spectra, 370-nm irradiation of *trans*-FK-11-X results in formation of 80% *cis* isomer with a concomitant 40% decrease in helical structure.[17] Thus, the 26% helix and 74% disordered secondary structures that are reported by the CD spectra after illumination reflect the average conformations of the 80% *cis* and 20% *trans* peptide ensembles. Assuming that the equilibrium percentages (66% helix/34% disordered) for the *trans* peptide are unperturbed in the population of peptides that does not undergo photoisomerization, then the 20% *trans* peptide population is expected to contribute 13% (20% of 66% helix) to the 26% helix observed after illumination. The 13% helix from the 20% *trans* peptide should be in equilibrium with 7% of the total 74% disordered structure observed after irradiation. The remaining 13% helix (26% − 13%) and 67% disordered (74% − 7%) structures must then be attributed to the 80% *cis*-FK-11-X that is formed upon photoisomerization, giving an equilibrium constant favoring unfolding of ~5. Because the observed relaxation rate (1/55 ns) is equal to the sum of the folding and unfolding rates ($k_f + k_u$), the equilibrium constant for unfolding ($K_{eq} = k_u/k_f$) can be used to approximate values of k_f and k_u for the *cis*-FK-11-X peptide. The folding and unfolding rates are thus calculated to be $\sim 3.0 \times 10^6$ s^{-1} (1/330 ns) and $\sim 1.5 \times 10^7$ s^{-1} (1/66 ns), respectively.

Several other phototriggers have been coupled with fast detection methods as a strategy to study peptide folding. Some of these include the photoactive aryl disulfide, CMB, and $[Rub_2m\text{-}OH]^{2+}$ groups used to study the helix−coil transition,[11,13,14] and the photoisomerizable azobenzene-based *p*-phenylazo-L-phenylalanine group for studies of the helix−sheet transition.[10] Unfortunately, many cross-linked peptide studies

have been confounded by problems such as a rapidly reversible photoinitiation event, low percentages of secondary structure change and low photoproduct yield of the photoactive group. However, it was possible to follow the peptide dynamics triggered by photoinduced charge generation in $[Rub_2m\text{-}OH]^{2+}$ and by photolysis of CMB.[13,14] The kinetic changes for the CMB peptide (35-residue villin headpiece subdomain, LSDEDFKAVFGMTRSAFANLPLWKQQNLKKEKGLF)[25] were probed with photoacoustic calorimetry (PAC) and photothermal beam deflection (PBD) methods, both of which are sensitive to volume changes.[13] Whereas the PBD data indicate that the folding process is complete within the 10-μs experimental dead time, the PAC data identified two kinetic phases, 100 and 400 ns, one of which is reported to be likely due to fast helix formation. The presence of one versus two kinetic phases in the results of the FK-11-X and the CMB studies may be due to the significant differences in the sequence and length of the peptides. However, without further characterization of their 100- and 400-ns processes a comparison is difficult. An interesting phototrigger introduced by Huang et al.[14] incorporates a $[Rub_2m\text{-}OH]^{2+}$ N-terminal cap in a 21-residue, alanine-based peptide (RuFs, $[Rub_2m\text{-}OH]^{2+}$-CONH-AAAAA$(AAARA)_3$A-$CONH_2$). Peptide folding was initiated by a metal-to-ligand charge transfer to form the long-lived (1−2 μs) excited state of $[Rub_2m\text{-}OH]^{2+}$ and probed by time-resolved infrared (TRIR) spectroscopy. The decay kinetics of RuFs were fit to two exponential processes with time constants of ∼220 and 524 ns, which were respectively correlated with helix formation and decay of the $[Rub_2m\text{-}OH]^{2+}$ excited state. Although a single-exponential process for the helix dynamics is consistent with the TRORD results, the time constant of 220 ns is slower than the 55-ns relaxation time observed for FK-11-X. However, the 220-ns relaxation is consistent with T-jump studies on similar 21-residue peptide systems (discussed below).

A single exponential relaxation for peptide helix unfolding in FK-11-X is also consistent with the results of several laser-induced T-jump peptide studies coupled with TRIR, fluorescence (TRFL), and UV resonance Raman (UVRS) probes, however, the 55-ns time constant is considerably faster. For example, Williams et al.,[26] Lednev et al.,[27] Thompson et al.,[28] Huang et al.,[29] and Werner et al.[30] report that the unfolding data for several slightly different 21-residue, alanine-based peptides can be fit well to a single-exponential decay with time constants of 160 ± 60 ns (28 °C), 180 ± 60 ns (37 °C), 220 ns (27 °C),[28b] 230 ± 40 ns (21 °C),[29b] and 120 ns (30 °C), respectively. When compared with the k_u values (5.7×10^5 s^{-1} (1/1750 ns) to 4.2×10^6 s^{-1} (1/240 ns)) reported by some of the above studies[26,27a] the k_u (1.5×10^7 s^{-1} (1/66 ns)) obtained in these TRORD studies is as much as 2 orders of magnitude faster. The k_f (3×10^6 s^{-1} (1/330 ns)) calculated for the TRORD data is both slower than the k_f (5.7×10^6 s^{-1} (1/175 ns))[31] suggested from studies by Williams et al.[26] and faster than the k_f (1.3×10^6 s^{-1} (1/760 ns)) reported by Lednev et al.[27a] The discrepancy between the folding rates observed by Williams et al. and Lednev et al. is unexpected because the 21-residue peptides studied are so similar. Lednev et al. suggest that the source of the disagreement arises from differences in the calculated equilibrium constants, with the IR static secondary structure measurements being less accurate. This explanation is supported by the subsequent demonstration that the steady-state melting curve for the peptide could be fit well to a "zipper model", with the resulting thermodynamic parameters being similar to those reported by Thompson et al.[28a] On the basis of these arguments the rate of folding for FK-11-X is considered to be faster than that for the 21-residue, alanine-based peptides.

Although the relaxation kinetics of thermally induced peptide unfolding are discussed largely in terms of a single exponential, most of these studies also report a second, faster (<20 ns) process. The identity of this <20-ns component remains controversial, but several ideas have been offered to explain its origin. From the T-jump TRIR[26] and UVRS[27b] studies on the Fs peptide (Suc-AAAAA-$(AAARA)_3$A-NH_2) and the AP peptide ($A_5(A_3RA)_3A$) the <10-ns and 14-ns processes, respectively, were attributed to a temperature-dependent spectral shift (possibly arising from solvation effects) that occurs without changes in the peptide conformation. The T-jump TRFL data on the W_1H_5-21 peptide (Ac-WAAAH$^+$-$(AAAR^+A)_3$A-NH_2) was described as being well fit to a single-exponential decay.[28b] However, the kinetic data could also be fit to two exponential processes, with the additional process having a much faster time constant of <20 ns. This time constant is similar to that in an earlier study by Thompson et al. where the helix−coil kinetics were probed with an N-terminal localized fluorophore in the MABA-bound peptide (MABA-AAAAA-$(AAARA)_3$-ANH_2).[28a] Based on a "kinetic zipper" model for the helix−coil transition this fast phase was attributed to redistribution of helix lengths. Finally, T-jump TRIR data on two D-Arg peptides, Ac-YGG-$(KAAAA)_3$-CO-D-Arg-$CONH_2$ and Ac-YGSPEA$_3$$(KAAAA)_2$-r-$CONH_2$, as well as on ^{13}C-labeled derivatives of the latter, were described by as many as three exponential processes.[29] The earliest of these processes is also limited by the rise time of the instrument and was discussed in terms of an instantaneous spectral shift, subnanosecond conformational changes, or the equilibration of helix lengths.

The faster time constant for the TRORD studies on the cyclic FK-11-X peptide versus the single-exponential component ($\tau \approx 200$ ns) reported by the T-jump studies on similar 21-residue peptides may have several explanations. First, it is possible that the differences in the peptide sequences and lengths contribute to faster relaxation kinetics for the FK-11-X peptide. Because the peptides in the T-jump experiments are broadly similar, comprising largely alanine residues, it would have been surprising had the time constants reported been greatly different. Clearly the possibility of multiexponential relaxation kinetics in helix unfolding cannot be ruled out until the origin of the

(25) McKnight, C. J.; Doering, D. S.; Matsudaira, P. T.; Kim, P. S. *J. Mol. Biol.* **1996**, *260*, 126.
(26) Williams, S.; Causgrove, T. P.; Gilmanshin, R.; Fang, K. S.; Callender, R. H.; Woodruff, W. H.; Dyer, R. B. *Biochemistry* **1996**, *35*, 691.
(27) (a) Lednev, I. K.; Karnoup, A. S.; Sparrow, M. C.; Asher, S. A. *J. Am. Chem. Soc.* **1999**, *121*, 8074. (b) Lednev, I. K.; Karnoup, A. S.; Sparrow, M. C.; Asher, S. A. *J. Am. Chem. Soc.* **2001**, *123*, 2388.
(28) (a) Thompson, P. A.; Eaton, W. A.; Hofrichter, J. *Biochemistry* **1997**, *36*, 9200. (b) Thompson, P. A.; Munoz, V.; Jas, G. S.; Henry, E. R.; Eaton, W. A.; Hofrichter, J. *J. Phys. Chem. B* **2000**, *104*, 378
(29) (a) Huang, C.-Y.; Klemke, J. W.; Getahun, Z.; DeGrado, W. F.; Gai, F. *J. Am. Chem. Soc.* **2001**, *123*, 9235. (b) Huang, C.-Y.; Getahun, Z.; Wang, T.; DeGrado, W. F.; Gai, F. *J. Am. Chem. Soc.* **2001**, *123*, 12111. (c) Huang, C.-Y.; Getahun, Z.; Zhu, Y.; Klemke, J. W.; DeGrado, W. F.; Gai, F. *Proc. Natl. Acad. Sci. U.S.A.* **2002**, *99*, 2788.
(30) Werner, J. H.; Dyer, R. B.; Fesinmeyer, R. M.; Andersen, N. H. *J. Phys. Chem. B* **2002**, *106*, 487.

(31) This value represents the folding rate calculated using a folding K_{eq} of 10, an observed time constant of 160 ns, and the relation that the observed relaxation rate is equal to the sum of the folding and unfolding rates. The folding rate is recalculated to be 5.7×10^6 s^{-1} (1/175 ns), which is an order of magnitude slower than the rate (6×10^7 s^{-1}) reported in ref 26.

fast, <20-ns component is understood; in fact, this process may be exclusively due to the alanine-based peptide. Still, even in these TRORD studies a process faster than 55 ns cannot be precluded because of the time resolution of the experiment. Although it is possible to fit a second exponential process to the TRORD data, the corresponding time constant is unstable, fluctuating between 600 ps and 8 ns.

A second explanation for the faster TRORD time constant is that the destabilizing effect of the *trans-to-cis* photoisomerization may be much greater than that caused by a T-jump. That is, the presence of a cross-linker leads to a lower barrier for unfolding than with a T-jump trigger. This arises from the lack of compatibility of the instantaneous *cis* photoproduct with the helical peptide, as suggested by the difference in *trans* and *cis* potential energies reported by Flint et al.[17] And finally, the most feasible explanation for faster kinetics is that the cyclic FK-11-X peptide experiences a narrower conformational distribution during the folding process. The constraint imposed by the presence of the cross-linker may define fewer possible pathways towards completion of folding to the native structure than for the unconstrained 21-residue peptides. Depending on how the cross-linker affects the peptide structure, the peptide may be limited with respect to the number of conformations it can sample from the top of the folding funnel, or the peptide may be "jump-started" into folding at a point on the funnel landscape where the number of pathways to the native-state structure is reduced. In either case, the cyclic peptide spends less time in the conformational search for a "correct" folding pathway.

Conclusions

The results of these TRORD studies indicate a 55 ± 6 ns time constant for the unfolding dynamics of the 16-residue FK-11-X peptide. Folding and unfolding rates are estimated to be $\sim 3.0 \times 10^6$ s^{-1} (1/330 ns) and $\sim 1.5 \times 10^7$ s^{-1} (1/66 ns), respectively, both of which are faster than the reported rates for several similar 21-residue, alanine-based peptides. The faster folding rate of this cyclic peptide compared to those observed for unconstrained peptides demonstrates the effect of limiting the initial peptide conformational heterogeneity. Differences in the rates may also be due in part to the trigger methods used to initiate peptide folding/unfolding.

The ability to finely control the helix content opens up a range of possibilities in the study of the protein-folding landscape. By engineering different peptides with either more or less "ruggedness" it should be possible to map out and investigate the complexities of peptide folding, such as the observed temperature dependence of the unfolding process intimated by T-jump triggered folding studies. The success of this cross-linking approach will allow questions about the temperature and solvent dependence of peptide dynamics, as well as questions about how peptide sequence and length influence folding/unfolding kinetics, to be addressed in a systematic manner.

Acknowledgment. We thank Drs. James W. Lewis, Robert A. Goldbeck, Istvan Szundi, John S. Winterle, and Vladimir N. Uversky for invaluable and thought-provoking discussions. G.A.W. acknowledges the support of the Natural Sciences and Engineering Research Council (NSERC) of Canada. J.R.K. was supported by an NSERC studentship. This work was also supported by National Institute of General Medical Sciences (NIH) Grant GM38549.

JA030277+